BioMetals (2005) 18:221–232
DOI 10.1007/s10534-005-0582-3

Signal role for activation of caspase-3-like protease and burst of superoxide anions during Ce^{4+}-induced apoptosis of cultured *Taxus cuspidata* cells

Zhi-Qiang Ge, Song Yang, Jing-Sheng Cheng & Ying-Jin Yuan*
Department of Pharmaceutical Engineering, School of Chemical Engineering and Technology, Tianjin University, Weijin Road 92#, Nankai District, Tianjin 300072, P.R. China;
**Author for correspondence (Fax: +86-22-27403888; E-mail: yjyuan@public.tpt.tj.cn)*

Received 14 September 2004; accepted 13 January 2005; Published online: March 2005

Key words: apoptosis, caspase-3-like protease, Ce^{4+}, superoxide anions, *Taxus cuspidata*

Abstract

The signal events of 1 mM Ce^{4+} ($Ce(NH_4)_2(NO_3)_6$)-induced apoptosis of cultured *Taxus cuspidata* cells were investigated. The percentage of apoptotic cells increased from 0.82% to 51.32% within 6 days. Caspase-3-like protease activity became notable during the second day of Ce^{4+}-treatment, and the maximum activity was 5-fold higher than that of control cells at the fourth day. When the experiment system was pretreated with acetyl-Asp-Glu-Val-Asp-aldehyde (Ac-DEVD-CHO) at 100 μM, caspase-3-like activity resulted in distinct inhibition by 70% and 77.3% after 3 and 4 days of induction. Furthermore, 100 μM Ac-DEVD-CHO partially reduced the apoptotic cells by 58.6% and 60.8% at day 4 and 5 respectively. Ce^{4+} induced superoxide anions ($O_2\cdot-$) transient burst, and the first peak appeared at around 3.7–4 h, the second appeared at about 7 h. Both $O_2\cdot-$ burst and cell apoptosis were effectively suppressed by application of diphenyl iodonium (NADPH oxidase inhibitor). Inhibition of $O_2\cdot-$ production attenuated caspase-3-like activation by 49% and 53.6% during day 3 and 4 respectively. In addition, a total of 15 protein spots changed in response to caspase-3-like protease activation were identified by two-dimensional gel electrophoresis. These results suggest that Ce^{4+} of 1 mM induces apoptosis in suspension cultures of *T. cuspidata* through $O_2\cdot-$ burst as well as caspase-3-like protease activation. The burst of $O_2\cdot-$ exerts its activity as an upstream of caspase-3-like activation. Our results also implicate that other signal pathways independent of an $O_2\cdot-$ burst possibly participate in mediating caspase-3-like protease activation.

Abbreviations: Ac-DEVD-AMC – acetyl-Asp-Glu-Val-Asp-aminomethylcoumarin; Ac-DEVD-CHO – acetyl-Asp-Glu-Val-Asp-aldehyde; DPI – diphenylene iodonium; PBS – phosphate buffered saline; PI – propidium iodide; REEs – rare earth elements; ROS – reactive oxygen species.

Introduction

The rare earth elements (REEs) are composed of 15 metallic elements which have similar chemical properties to each other. Cerium is an important rare earth element and the several compounds of cerium have been used in clinical applications. In recent years, it has been reported that applying cerium compounds to plants resulted in obviously biological effects on plant growth and development. Floral initiation and reproductive growth of *Arabidopsis thaliana*, as well as, increased pollen germination and pollen tube growth was documented (He & Loh 2000; Sun *et al*. 2003).

In our previous studies, the application of Ce^{4+} ($Ce(NH_4)_2(NO_3)_6$), an important compound of cerium, to suspension cultures of *Taxus cuspidata* has been found to be very effective for strengthening taxol biosynthesis and release than other rare earth ions (La^{3+} and Ce^{3+}) (Yuan *et al*. 1998).

This metallic elicitor induced not only the production and release of Taxol, but also apoptosis (Ge *et al*. 2002). After discovering that the enhancement of taxol biosynthesis was accompanied by apoptosis in suspension cultures of *T. cuspidata*, it became imperative to understand the signal regulation of Ce^{4+}-induced apoptosis.

Programmed cell death (PCD) or apoptosis is a genetically controlled process that is essential in cell development, maintenance of homeostasis and stress-related responses (Ellis *et al*. 1991). Recent studies revealed that morphological and biochemical hallmarks of apoptosis, including cell shrinkage, chromatin condensation and DNA laddering, were similar in animal and plant cells (Ryerson & Heath 1996; Beers 1997). The rapid production of reactive oxygen species (ROS), which include superoxide anion ($O_2\cdot-$), hydrogen peroxide (H_2O_2) and hydroxyl radicals ($OH\cdot$) by plant cells, is one of the most striking events that occur during the early phases following pathogen attack and abiotic stress. Several sources identified H_2O_2 as a signal molecule in the induction of plant apoptosis (Buckner *et al*. 2000; Dat *et al*. 2000). In contrast, $O_2\cdot-$ also is a key regulator of induction of apoptosis (Jabs *et al*. 1997; Overmyer *et al*. 2000). Furthermore, abiotic elicitor-defense responses were associated with ROS-mediated systems base on the plasma-membrane-bound NADPH oxidase complex (Overmyer *et al*. 2000; De Dong *et al*. 2002). Our previous results have shown that Ce^{4+}-induced $O_2\cdot-$ burst could mediate taxol production by activating the NADPH oxidase complex (Yuan *et al*. 2002b).

Although previous reports have suggested an involvement of caspase-like proteases in plant systems (Del Pozo & Lam 1998), an important role of caspase-like protease has been only recently recognized (Elbaz *et al*. 2002; Chichkova *et al*. 2004). It was discovered that some specific inhibitors of animal caspase could effectively prevent the induction of apoptosis in tomatoes (De Jong *et al*. 2000), tobacco (Mlejnek & Procházka 2002), and soybean (Zuppini *et al*. 2003) suspension cell cultures in response to various elicitors. Recently, many arguments focused on the signal events of oxidative burst and caspase activation in animal cells. Some evidence indicated that ROS production determined the activation of downstream caspases in human leukemia cells (Chung *et al*. 2003), whereas others showed that generation of ROS could require upstream caspase-3 activation during the anticancer drugs-induced apoptosis (Simizu *et al*. 1998). In *Arabidopsis* suspension cells, Clarke A *et al*. reported that nitric oxide- and H_2O_2-induced apoptosis was inhibited by the caspase-1 inhibitor and suggested that the release of NO and H_2O_2 could activate caspase proteases (Clarke *et al*. 2000). However, to date, few evidence indicates the signal sequence of $O_2\cdot-$ burst and caspase-like protease activation in plant systems.

In this study, we investigate the role of activation of caspase-3-like protease and burst of $O_2\cdot-$ in Ce^{4+}-induced apoptotic process, and try to further demonstrate the signal sequence between caspase-3-like protease activation and $O_2\cdot-$ burst. In addition, the changes of the protein expression profile associated with caspase-3-like protease activation are identified.

Materials and methods

Chemicals

Ammonium ceric nitrate ($Ce(NH_4)_2(NO_3)_6$) was purchased from Aldrich. Cerium nitrate hexahydrate ($Ce(NO_3)_3 \cdot 6H_2O$), propidium iodide (PI), Hoechst 33342, diphenylene iodonium (DPI) and Coomassie Blue R250 were purchased from Sigma. Ac-DEVD-AMC and Ac-DEVD-CHO were purchased from Calbiochem. DTT, Chaps and PMSF were purchased from Roche. Isoelectric focusing (IEF) gel was from Amersham Pharmacia. All other chemicals were of analytical grade and obtained commercially.

Cell culture

The cell line from the young stems of *Taxus cuspidata* was subcultured on solid B5 medium at 25 °C in dark (Ge *et al*. 2002). Cell suspensions were cultured every 10 days for a total of five generations in fresh modified B5 medium containing sucrose (25 g l^{-1}), naphthylacetic acid (2 mg l^{-1}) and 6-benzyl aminopurine (0.15 mg l^{-1}). The suspensions were maintained in 250 ml shake flasks at 25 °C with continuous shaking (110 rpm) in the dark. The pH of the medium was adjusted to 5.8 with 0.1 M NaOH or 0.1 M HCl. Ce^{4+} ($Ce(NH_4)_2(NO_3)_6$) and Ce^{3+} ($Ce(NO_3)_3 \cdot 6H_2O$)

respectively were dissolved in distilled water to obtain a 0.5 M stock solution. 100 μl stock solutions, in exponential growing stage (at the tenth day), were added to the culture system with 50 ml of medium to make a final concentration of 1 mM Ce^{4+} and Ce^{3+}. Ac-DEVD-CHO and DPI were dissolved in DMSO. Various amounts of Ac-DEVD-CHO and DPI were applied to the culture system 2 h prior to the addition of Ce^{4+}. In all experiments, the final concentration of DMSO was approximately 0.1% (v/v).

Hoechst 33342-propidium iodide co-staining

The cells were stained with fluorescent dyes, Hoechst 33342 and PI, following the method of Yuan *et al*. (Yuan *et al*. 2002a). The percentage of apoptotic cells was estimated from at least 500 cells randomly counted at different time points. The experimental data were measured as the means ± S.E.M of at least three independent experiments.

Assay of DNA fragments

Total DNA was extracted following the method of Dellaporta *et al*. with a slight modification (Dellaporta *et al*. 1983). Fresh cells were grounded in liquid N_2 with mortar and pestle and powder were dissolved in 500 μl lysis buffer (2% (w/v) CTAB, 10 mM Tris–HCl pH 8.0, 20 mM EDTA, 1.4 mM NaCl and 2% (v/v) β-mercaptoethanol) at 65 °C for 30 min and centrifuged at 12 000 *g* for 20 min. The water phase was extracted with chloroform/isoamyl alcohol (24:1, v/v). The supernatant was mixed with pellet buffer (1% (v/v) CTAB, 50 mM Tris–HCl pH 8.0 and 10 mM EDTA) at 65 °C for 30 min and collected by centrifugation at 3000 *g* for 10 min. The pellets were re-suspended in 0.5 ml high-salt buffer (10 mM Tris–HCl pH 8.0, 1 mM EDTA and 1 M NaCl). DNA were precipitated by two volume of ethanol at −20 °C for 2 h and centrifuged, washed with 75% (v/v) ethanol and then dried at 37 °C. The dried DNA were dissolved in 30 μl TE buffer (10 mM Tris–HCl pH 8.0, 1 mM EDTA) containing RNase A (100 μg ml^{-1}) and incubated at 37 °C for 30 min. The DNA samples were run on 1.5% (w/v) agarose gel stained with ethidium bromide and illuminated under ultraviolet (GDS-8000, UVP).

Measurement of caspase-3-like protease activity

Caspase-3-like protease activity was assayed following the method of Mlejnek *et al*. with a slight modification (Mlejnek & Procházka 2002). Fresh cells were grounded in liquid N_2 with mortar and pestle. The cell powder were lysed in caspase lysis buffer (50 mM Hepes pH 7.2, 1 mM EDTA, 0.2% Chaps, 5 mM DTT, 20% glycerol, 1 mM PMSF) at 4 °C for 30 min. Lysates were centrifuged at 28 000 *g* for 30 min and the upper cytosol was collected for measurement. An appropriate volume of cytosol (200–300 μg of total protein) was mixed with 500 μl of caspase assay buffer (50 mM Pipes-KOH pH 7.2, 5 mM EGTA, 2 mM $MgCl_2$, 5 mM DTT) and reactions were initiated by adding a specific substrate (Ac-DEVD-AMC, 100 μM). Samples were incubated at 30 °C for 2 h and the fluorescence was measured using a fluorescent spectrophotometer (Varian, CARY Eclipse) at an excitation/emission wavelength of 380/445 nm. The relative AMC fluorescence of caspase-3-like protease activities were determined by the formula: $\Delta\lambda_{445} = \lambda_{445}$(enzyme extract with substrate) $-\lambda_{445}$(enzyme extract without substrate) $-\lambda_{445}$(substrate added to caspase lysis buffer without enzyme extract). The absolute value of enzymatic activities was determined by standardizing to the quantity of total proteins present in the sample and reaction time. The experiment data were measured as means ± S.E.M of at least three independent experiments.

Determination of $O_2\cdot-$

Superoxide anions were assayed following the method of Han *et al*. with a slight modification (Han & Yuan 2004). Cell suspension cultures (0.5 ml) were mixed with 1 ml of 1 mM hydroxylammonium chloride and 0.5 ml of 50 mM phosphate buffer (pH 7.8), and the mixture was incubated at 25 °C for 60 min. Then 1ml sulphanilamide (17 mM) dissolved in 30% (w/w) acetic acid and 1ml of naphthalene diamine dihydrochloride (7 mM) were added and the mixture was incubated at 25 °C for 20 min. The absorbance was measured at 530 nm using a spectrophotometer (UNIC, UV-4802). Calibration curve of OD530 against NO_2^- concentration was established ($r^2 = 0.9968$). The concentration of $O_2\cdot-$ was calculated as twice of that of

NO_2^- based on the following reaction: $2O_2\cdot- + H^+ + NH_2OH \rightarrow H_2O_2 + H_2O + NO_2^-$. The experimental data was based on cell dry weight determined at the end of the measurement in order to correct variations between samples, and measured as the means ± S.E.M of at least three independent experiments.

Extraction of proteins and two-dimensional gel electrophoresis of proteins

Fresh cells (1 mg) were grounded in liquid N_2 with mortar and pestle, and powder (0.2 g) were dissolved in 0.5 ml lysis buffer (8 M urea, 4% (m/v) CHAPS, 40 mM Tris-base and 1 mM PMSF) at 4 °C for 2 h. The mixture was centrifuged at 15 000 *g* for 30 min and the supernatant was mixed with three volume of ice-cold acetone at −20 °C for 2 h. The mixture was centrifuged at 10 000 *g* for 20 min and the precipitate was freeze-dried. The dried cytosolic proteins were dissolved in 100 μl rehydration buffer (8.0 M urea, 2.0% (m/v) Chaps, 20 mM DTT, 0.5% (v/v) IPG buffer and small amounts of bromphenol blue). 2-D gel electrophoresis of proteins was performed on the Hoefer DALT Vertical System. IEF gels (pH 4–7, 18 cm long) were re-hydrated with the proteins (1000 μg), dissolved in 350 μl rehydration buffer and focused on an IPGphor apparatus. The first dimension electrophoresis was run using the following conditions: 30 V for 12 h, 500 V for 1 h, 1000 V for 1 h, 8000 V for 8 h. Then, the IPG strips were incubated in a SDS equilibration buffer (50 mM Tris–HCl of pH 8.8, 6 M urea, 30% (v/v) glycerol, 2% (m/v) SDS, 1% (m/v) DTT, trace of bromophenol blue) for 15 min. After being equilibrated, the proteins were separated on 12.5% SDS-PAGE gels and stained with Coomassie Blue R250 in 50% methanol and 10% acetic acid. The 2-D gel image was analyzed using the Image Master 2-D software.

Statistics

The experimental points represent the mean values from at least three independent experiments ± standard error of the mean (S.E.M). The significance of differences between experimental conditions was determined using two independent sample *t*-tests. A *P* value less than 0.05 was considered to be statistically significant.

Results

Apoptotic cells induced by Ce^{4+}

At various cultivation stages, apoptotic cells were almost not detected in controls (Figure 1). The percentage of apoptotic cells increased after 3 days of Ce^{4+} treatment (** $P < 0.001$) and gradually reached a maximum of 51.32% at the sixth day (** $P < 0.001$). The percentage of apoptotic cells at the seventh day showed a decrease from 51.32% to 46.6% ($P < 0.05$). In a parallel set of experiments, we treated cells with 1 mM Ce^{3+}, which could not induce cell apoptosis (the percentage of apoptotic cells at the sixth day was only 3.32%).

Caspase-3-like protease activation by Ce^{4+} and Caspase-3 inhibitor suppresses Ce^{4+}-induced apoptosis

To identify the role of caspase-3-like protease activation during cellular apoptosis, a substrate of caspase-3 (Ac-DEVD-AMC) was added to protein extracts prepared from Ce^{4+}-induced cells at various time points. As can be seen in Figure 2a, the comparison of caspase-3-like protease activity from Ce^{4+}-induced and control cells allowed quantification of the increased protease activity. Caspase-3-like protease activity became notable

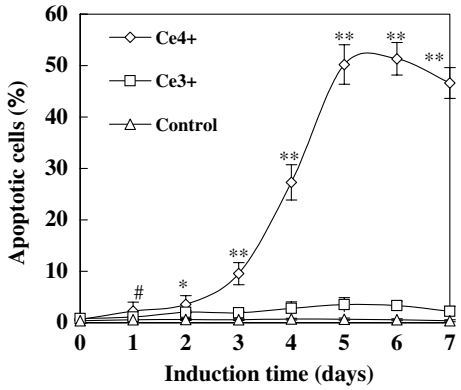

Figure 1. Induction of apoptosis by Ce^{4+}. Ce^{4+} of 1 mM and Ce^{3+} of 1mM respectively were added at 10 day of the cultivation. The percentage of apoptotic cells was estimated using co-staining with Hoechst 33342 and PI, and at least 500 cells were examined in one experiment. Data represent the means ± S.E.M of three independent experiments. Ce^{4+}-induced cell compared with the control cell (* $P < 0.05$, ** $P < 0.001$, # $P > 0.05$).

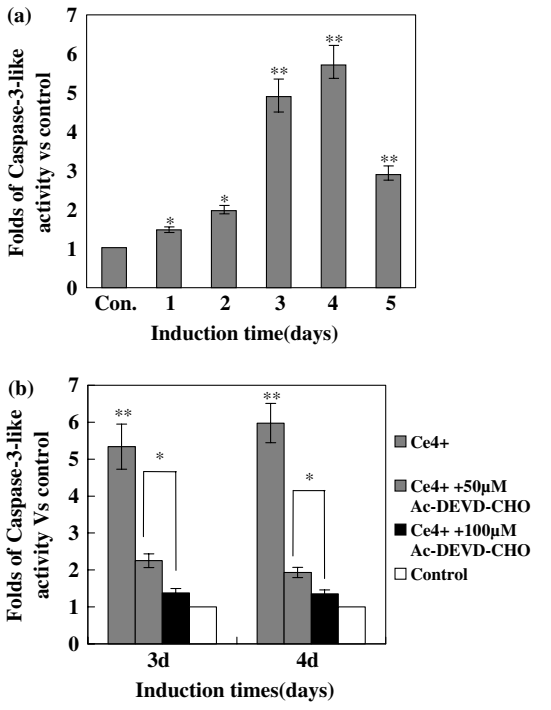

Figure 2. Activation of caspase-3-like protease in Ce^{4+}-induced apoptosis of suspension cultures of *Taxus cuspidata*. Data represent the means ± S.E.M of at least three independent experiments. (a) Caspase-3-like protease activities were detected at the different time points. Ce^{4+}-induced cell compared with the Control cell (* $P < 0.05$, ** $P < 0.001$). Con. = 215.42 ± 19.18 nmol mg protein^{-1} .h^{-1}. (b) Effect of caspase-3 inhibitor on caspase-3-like protease activities. Ac-DEVD-CHO of 100 and 50 μM were applied to cell cultures 2 h before the addition of 1 mM Ce^{4+}. Caspase-3-like protease activities were detected at the third and fourth days. Ce^{4+}-induced cell with 100 μM Ac-DEVD-CHO compared with Ce^{4+}-induced cell alone (** $P < 0.001$). Ce^{4+}-induced cell with 100 μM Ac-DEVD-CHO compared with Ce^{4+}-induced cell with 50 μM Ac-DEVD-CHO (* $P < 0.05$). Con. 3d = 196.65 ± 12.73 nmol mg protein^{-1} h^{-1}, Con. 4d = 208.72 ± 22.10 nmol mg protein^{-1} h^{-1}.

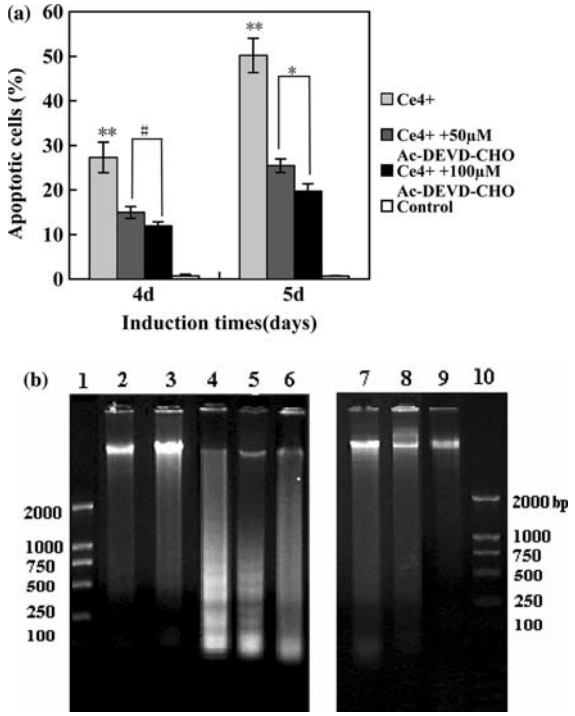

Figure 3. Inhibition of Ce^{4+}-induced apoptosis by caspase-3 inhibitor. Ac-DEVD-CHO of 100 and 50 μM were applied to cell cultures 2 h before the addition of 1 mM Ce^{4+}. (a) The percentage of apoptotic cells was estimated using co-staining with Hoechst 33342 and PI, and at least 500 cells were examined in one experiment. Data are the means ± S.E.M of at least three independent experiments. Ce^{4+}-induced cell with 100 μM Ac-DEVD-CHO compared with Ce^{4+}-induced cell alone (** $P < 0.001$). Ce^{4+}-induced cell with 100 μM Ac-DEVD-CHO compared with Ce^{4+}-induced cell with 50 μM Ac-DEVD-CHO (* $P < 0.05$, # $P > 0.05$). (b) DNA was isolated from control cells (control-line 2), Ce^{4+}-treatment alone (4d-line 3, 5d-line 4, 6d-line 5, 7d-line 6) and Ce^{4+}-treated cells with 100 μM Ac-DEVD-CHO (5d-line 7, 6d-line 8, 7d-line 9). Molecular weight markers are line 1, 10. Results are representative of three independent experiments.

after 2 days of treatment (* $P < 0.05$) and gradually increased reaching a peak level at day 4. The maximum activity was 5-fold higher than that of control cells (** $P < 0.001$). To further elucidate caspase-3-like protease function, we added two different concentrations of caspase-3 inhibitor (Ac-DEVD-CHO) to the cultured system. As expected, caspase-3-like activity was significantly inhibited. Inhibition at a rate of 70% and 77.3% resulted following addition of 100 μM Ac-DEVD-CHO at days 3 and 4 respectively (** $P < 0.001$) (Figure 2b). Also, activity decreased 57.8% and 67.6% with 50 μM Ac-DEVD-CHO addition (** $P < 0.001$) (Figure 2b). Furthermore, 100 and 50 μM concentrations of Ac-DEVD-CHO reduced in part the number of apoptotic cells respectively by 58.6% and 45.2% at day 3 and by 60.8% and 49.1% at day 4 (** $P < 0.001$, * $P < 0.05$, # $P > 0.05$) (Figure 3a). DNA assays revealed a large DNA fragment at about 25 kb in the control. A visible DNA ladder appeared at day 5, while a more distinct ladder pattern was observed at day 6 (Figure 3b). However, the DNA ladder in treated cells with 100 μM Ac-DEVD-CHO was much less distinct than in cells treated with Ce^{4+} alone (Figure 3b).

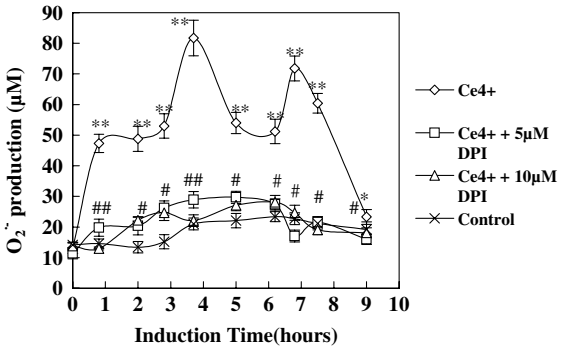

Figure 4. Time course of burst of $O_2 \cdot -$ induced by Ce^{4+} and effect of DPI on production of $O_2 \cdot -$. Ce^{4+} of 1 mM was added at 10 day of the cultivation. DPI of 10 and 5 μM were applied to cell cultures 2 h before the addition of 1 mM Ce^{4+}. Data represent the means ± S.E.M of at least three independent experiments. Ce^{4+}-induced cell compared with the control cell (* $P < 0.05$, ** $P < 0.001$). Ce^{4+}-induced cell with 10 μM DPI compared with Ce^{4+}-induced cell with 5 μM DPI (# $P > 0.05$, ## $P < 0.05$).

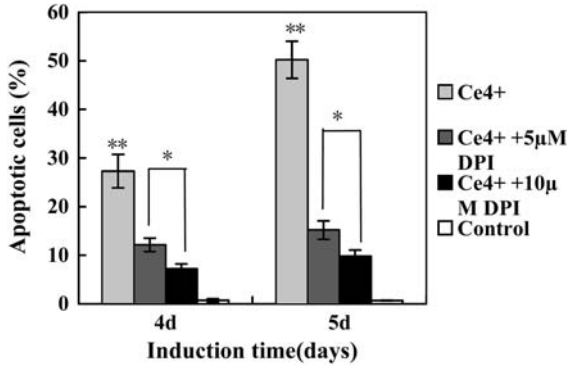

Figure 5. Inhibition of Ce^{4+}-induced apoptosis by DPI. DPI of 10 and 5 μM were applied to cell cultures 2 h before the addition of 1 mM Ce^{4+}. The percentage of apoptotic cells was estimated using co-staining with Hoechst 33342 and PI at the fourth and fifth days, and at least 500 cells were examined in one experiment. Data represent the means ± S.E.M of three independent experiments. Ce^{4+}-induced cell with 10 μM DPI compared with Ce^{4+}-induced cell alone (** $P < 0.001$). Ce^{4+}-induced cell with 10 μM DPI compared with Ce^{4+}-induced cell with 5 μM DPI (* $P < 0.05$).

Burst of $O_2 \cdot -$ induced by Ce^{4+}

As illustrated in Figure 4, a significant dynamic burst of $O_2 \cdot -$ was observed in *Taxus cuspidata* cells treated with Ce^{4+}. Detailed analyses of time-dependent increases in $O_2 \cdot -$ levels indicated that the first peak appeared at around 3.7–4 h, the second peak at about 7 h, and then $O_2 \cdot -$ production declined at 9 h compared to the control level. The amount of the first peak was 5.75-fold higher than that of the control cells, and the second peak was 5.06-fold higher (** $P < 0.001$). In our experiments, we also measured $O_2 \cdot -$ concentrations at day 6 and 7. It was found that $O_2 \cdot -$ concentrations had declined back to control values ($O_2 \cdot - < 20$ μM). The concentration of $O_2 \cdot -$ was reduced to less than 30 μM with the addition of 5 μM DPI, and 10 μM DPI produced a more effective inhibition (# $P > 0.05$, # # $P < 0.05$). Figure 5 showed DPI significantly attenuated the cellular apoptosis (** $P < 0.001$). Ten micromolar DPI caused a reduction of apoptotic cells by 73.6% and 80.5% at days 4 and 5 respectively, whereas 5 μM DPI resulted in a reduction of 55.6% and 71.8% (* $P < 0.05$).

Caspase-3-like protease activation not depend on burst of $O_2 \cdot -$ entirely

To investigate a hypothesis that burst of $O_2 \cdot -$ acted as a mediator of activation of caspase-3-like protease, DPI was added to cultured cells 2 h before the application of Ce^{4+}. As shown in Figure 6, 10 μM DPI caused a reduction of Ce^{4+}-activated caspase-3-like protease by 49% and 53.6% after 3 and 4 days of treatment respectively, and 5 μM DPI reduced by 41.8% and 44.4% (* $P < 0.05$). The *t*-tests also indicated that the inhibition effect of 10 or 5 μM DPI on caspase-3-like protease was significant at a probability level (** $P < 0.001$).

The expression of different proteins associated with caspase-3-like protease activation identified by two-dimensional gel electrophoresis

To further identify downstream signal molecules in response to caspase-3-like protease activation, we compared the proteome of Ce^{4+}-induced cells alone at day 5 with that of Ce^{4+}-induced cells in the presence of 100 μM Ac-DEVD-CHO. We detected more than 600–700 proteins spots on 2-D gels, and found 15 changed spots across two gels in Figure 7(a2) and (a3) which were distributed in p*I* 5.8–6.6 and their molecular masses ranged 18.0–45.0 kDa. Expressed protein abundance of eight spots (A, B, C, D, I, J, K, P spots) were decreased compared with Ce^{4+}-induced alone and other seven spots protein (E, F, G, H, L, M, N spots) were increased (Figure 7b). Meanwhile, we also

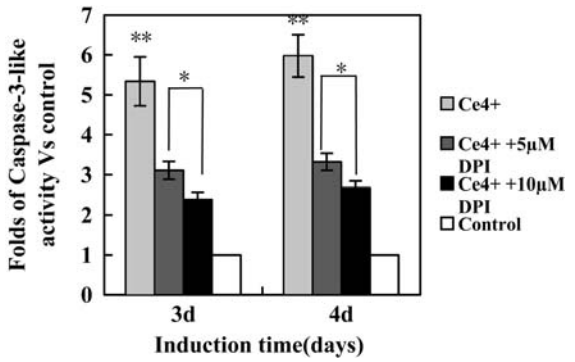

Figure 6. The signal sequence between caspase-3-like protease activation and burst of $O_2 \cdot -$. DPI of 10 and 5 μM were applied to cell cultures 2 h before the addition of 1 mM Ce^{4+}. Caspase-3-like protease activities were detected at the third and fourth days. Data are the means ± S.E.M of three independent experiments. Ce^{4+}-induced cell with 10 μM DPI compared with Ce^{4+}-induced cell alone (** $P < 0.001$). Ce^{4+}-induced cell with 10 μM DPI compared with Ce^{4+}-induced cell with 5 μM DPI (* $P < 0.05$). Con. 3d = 196.65 ± 12.73 nmol mg protein^{-1} h^{-1}, Con. 4d = 208.72 ± 22.10 nmol mg -protein^{-1} h^{-1}.

compared 15 changed spots above with that of the control cells (Figure 7(a1)). Ac-DEVD-CHO effectively prevented caspase-3-like protease-activated alterations of 15 spots protein. Protein abundance of 12 of the 15 changed spots in Ce^{4+} -induced cells with 100 μM Ac-DEVD-CHO showed some similarity with that of the control. For example, K spot identified was increased after Ce^{4+} treatment, but the expression of this protein was approximately decreased to the level of the control cells due to addition of caspase-3 inhibitor. The similar inhibition was also observed in other 11 spots (A, E, F, G, H, I, J, L, M, N, P). The change of B, C, and D spots differed from these 12 protein spots.

Discussion

Our previous studies have demonstrated that different elicitors could result in the apoptosis of suspension culture of *Taxus chinensis* and *Taxus cuspidata* (Li *et al*. 2002; Qiao *et al*. 2002). Wätjen *et al*. indicated that 1–100 μM Cd^{2+} or high concentrations of Zn^{2+} (>150 μM) caused apoptosis of C6 glioma cells (Wätjen *et al*. 2002). In our present works, using Ce^{4+} as metallic elicitor, we analyzed the changes of percentage of apoptotic cells in suspension culture of *T. cuspidata*. After being exposed to 1 mM Ce^{4+} within 7 day, the number of apoptotic cells was significantly enhanced compared with that of Ce^{3+}-treated cells and control cells (Figure 1). A decrease in the number of apoptotic cells at the seventh day from 51.32% to 46.6% reflected the transformation of cells from apoptosis to the dying state, which resulted from an increase 4.72% of necrotic cells. The effects of Ce^{4+}-treated *T. cuspidata* cells on apoptosis could be partially attributed to the particularity of this compound, including its high redox (Φ^{θ} Ce^{4+}/Ce^{3+} = 1.4430).

Recent work has indicated that a definite role for caspase-3-like protease activation has been identified in the hypersensitive-response of tobacco leaves (Del Pozo & Lam 1998), the heat shock-induced apoptosis of tobacco suspension cells (Tian *et al*. 2000), and the apoptosis of megagametophyte cells after germination of *Picea glauca* seeds (He & Kermode 2003). Furthermore, evidence from caspase-like purification indicated that this plant enzyme during the HR triggered by TMV and human caspase-3 protease have partially overlapping protein sequences (Chichkova *et al*. 2004). In our case, activities of caspase-3-like protease were first clearly detected after 2 days of Ce^{4+} treatment, and a maximum activity appeared at day 4 (Figure 2a). The activated caspase-3-like protease through a complex activation cascade led to the activation of other proteases and cleaved various targeted proteins. These activated signal molecules at last caused an increase of apoptotic cells from 3.56% at day 2 to 51.32% at day 6 (Figure 1). Our results further showed 100 or 50 μM Ac-DEVD-CHO significantly blocked caspase-3-like protease activation (Figure 2b) and Ac-DEVD-CHO prevented in part cell apoptosis (Figure 3a and b). Since the plant cellular wall could tend to adsorb a certain amount of Ac-DEVD-CHO applied to the suspension cultures, a higher concentration of inhibitor (100 μM) was more efficient than 50 μM inhibitor for researching the apoptotic process. It was interesting that although caspase-3-like protease activation was an essential event of Ce^{4+}-induced apoptotic pathway, caspase-3 inhibitor was not sufficient to suppress the apoptosis of *T. cuspidata* cells. These results implicated that different signal pathways might be activated in Ce^{4+}-treated cells. It has been reported that a caspase-independent signaling pathway was involved in apoptosis of

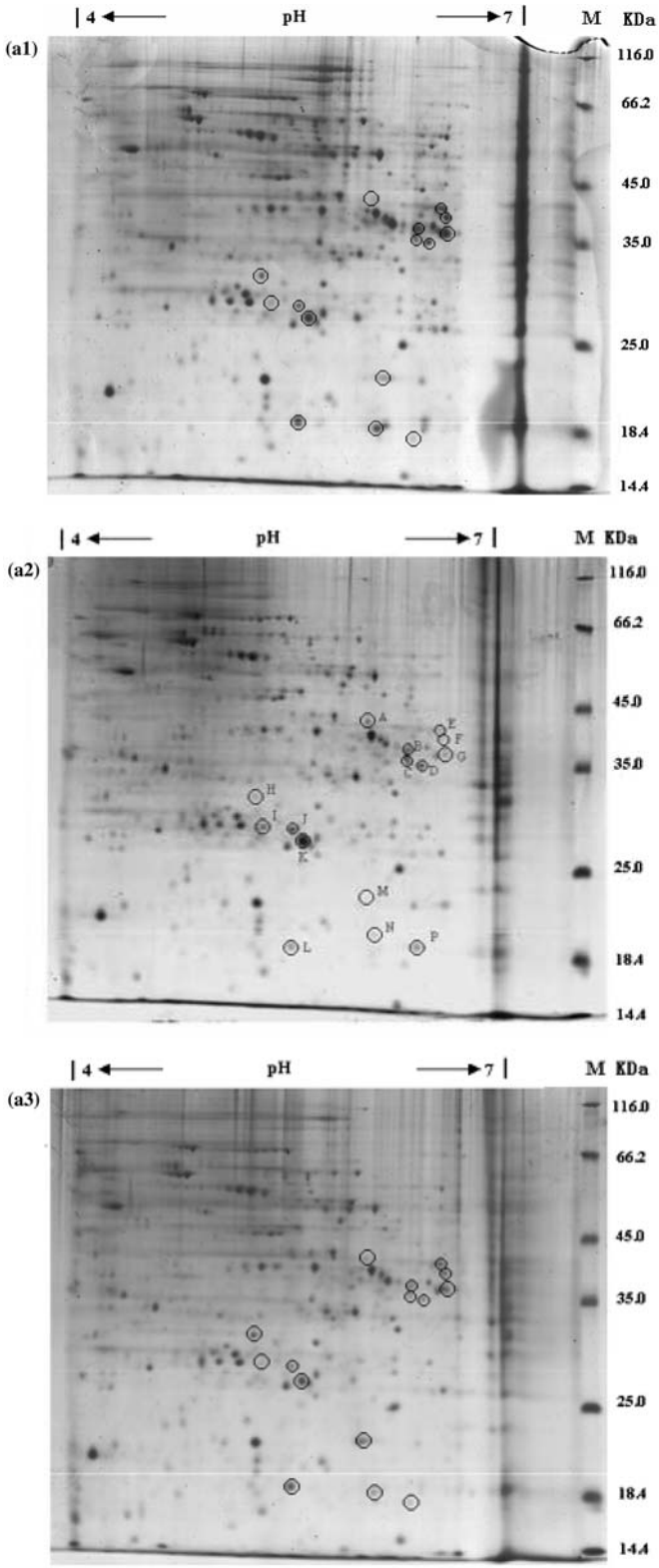
(a1)
4
pH
7
M
KDa
116.0
66.2
45.0
35.0
25.0
18.4
14.4
(a2)
4
pH
7
M
KDa
116.0
66.2
45.0
35.0
25.0
18.4
14.4
A
B
C
D
E
F
G
H
I
J
K
L
M
N
P
(a3)
4
pH
7
M
KDa
116.0
66.2
45.0
35.0
25.0
18.4
14.4

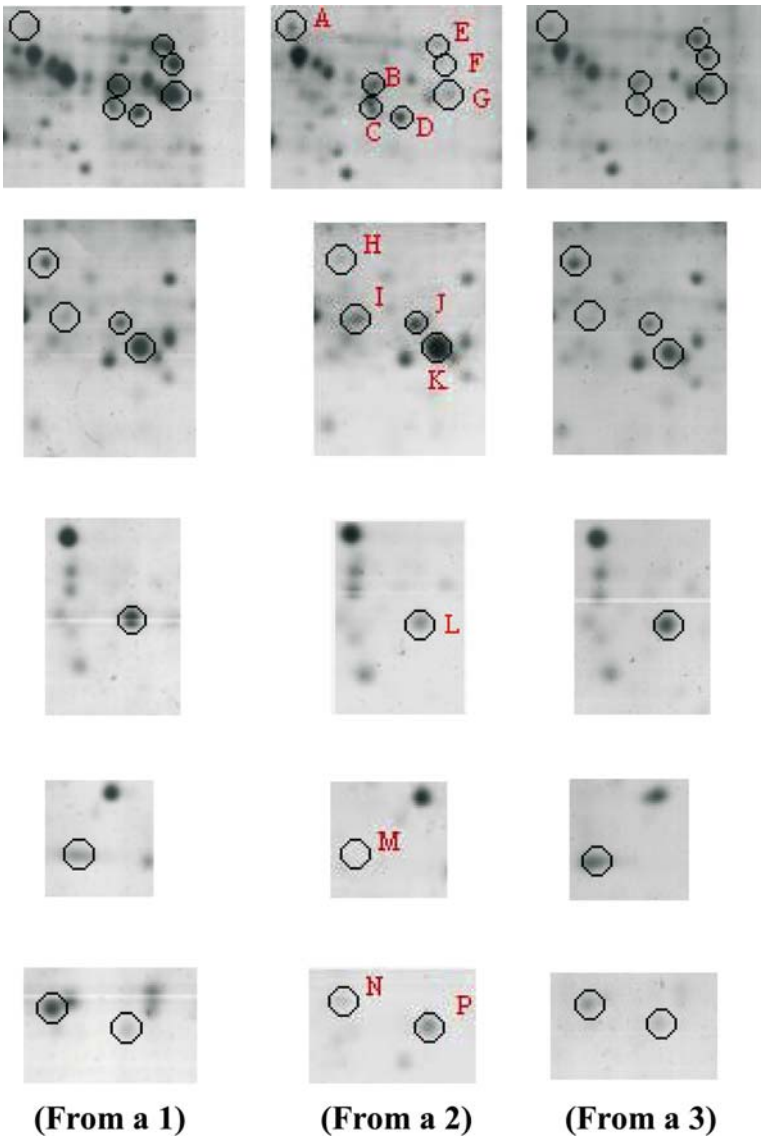

Figure 7. The expression of 15 different proteins (A–P spots) induced by Ce^{4+} depend upon caspase-3-like protease activation. Results are representative of three independent experiments. (a) The proteome of Ce^{4+}-induced cells alone at day 5 (a2) was compared with that of Ce^{4+}-induced cells in the presence of caspase-3 inhibitor AC-DEVD-CHO of 100 μM (a3) and the control cells (a1). Total cell lyates (1000 μg) were subjected to 2-D gel electrophoresis, and stained by Coomassie R250. The first-dimension electrophoresis between pH 4 and 7 of entire gel images was shown on top of the gel, and molecular mass marker for 12.5% SDS-PAGE in the second dimension was shown on the right side. The original gel size was 250 × 180 × 1 mm. (b) Enlargement of gel segments containing eight up-regulated proteins (A, B, C, D, I, J, K, P spots) and other seven down-regulated proteins (E, F, G, H, L, M, N spots).

Arabidopsis cells, which was mediated by AIF (apoptosis-inducing factor)-like associated with mitochondria (Balk *et al.* 2003). Moreover, the activation of other cysteine proteases or caspase-like protease involved in apoptosis of Ce^{4+}-induced could be another reason for the failure of Ac-DEVD-CHO inhibition. Some evidences have proposed that caspase-1-like or caspase-6-like protease instead of caspase-3-like protease was a critical role during the apoptosis in tobacco cells (Chen *et al.* 2000; De Jong *et al.* 2002), and other cysteine proteases without existing caspase-like protease activities also played a key role in oxidative stress-induced apoptosis of soybean cells (Solomon *et al.* 1999). Various apoptosis-inducing signal activations and trans-

ductions reflect the differences of apoptotic mechanism in the different model systems. While it was currently unclear how Ce^{4+} directly activated caspase-3-like protease and how caspase-3-like protease mediated apoptosis, it was likely to that caspase-3-like activation was very important for cell apoptosis of suspension culture of *T. cuspidata*.

Recently, it has been reported there was a biphasic oxidative burst in response to an avirulent microbial pathogen (Levine *et al*. 1994; Jabs *et al*. 1997). Interestingly, double peaks of $O_2\cdot-$ also were observed in our results. The first peak occurred rapidly at about 3.7–4 h, the second weak peak at 7 h (Figure 4). It was presumed that the characteristics resemble the manner of oxidative burst in avirulent pathogen induction. The addition of DPI (NADPH-oxidase inhibitor) strongly suppressed Ce^{4+}-induced $O_2\cdot-$ burst and cell apoptosis (Figures 4 and 5). In mammalian cells, some heavy metal ions (Fe^{2+}, Cu^{2+} and Co^{2+} *et al*.) initiated oxidative damage by enhancing the release of ROS through Fenton-like reactions (Stohs & Bagchi 1995), whereas Gd^{2+} induced apoptosis of C6 glioma cells indirectly through inhibition of antioxidant enzymes (Wätjen & Beyersmann 2004). In our case, it was concluded that the production of $O_2\cdot-$ was mainly due to NADPH-oxidase activity and an early burst of $O_2\cdot-$ was a prerequisite for upstream apoptotic signal activation. Ten micromolar DPI failed to fully inhibit caspase-3-like protease activation (Figure 6), but successfully suppressed the apoptosis of *T. cuspidata* cells (Figure 5). Our findings implicated that the role of caspase-3-like protease in Ce^{4+}-induced cells was complex. It is necessary to mention that caspase-like proteases have been reported in tomato suspension cultures as upstream signals mediating the release of H_2O_2 (De Dong *et al*. 2002). However, our results showed an opposite viewpoint that burst of $O_2\cdot-$ triggered activation of caspase-3-like protease in Ce^{4+}-induced apoptosis. Furthermore, caspase-3-like protease activation in part depended on the generation of $O_2\cdot-$, and other signal cascades independent of $O_2\cdot-$ possibly participated in regulating caspase-3-like protease. Indeed, the addition of DPI completely prevented the early production of $O_2\cdot-$ and partially prevented the late responses such as caspase-3-like activation. In mammalian cells, the case for the relation between generation of ROS and activation of caspase-3-like was also controversial. Early evidences have shown that activation of caspase-3 protease by anticancer drugs could cause generation of H_2O_2 through NADPH oxidase complex (Simizu *et al*. 1998). However, recent results emphasized that ROS, which were upstream of caspase activation, acted at an early stage of apoptosis (Chung *et al*. 2003; Yu *et al*. 2004). In the present study, our results proposed the key role of $O_2\cdot-$ burst and caspase-3-like protease activation, and revealed a positive correlation between $O_2\cdot-$ and caspase-3-like protease events leading to apoptosis of *T. cuspidata* cells.

Although different protein expression associated with caspase activation in different animal cells have been reported (Jin *et al*. 2003; Kaji *et al*. 2003), few data have been demonstrated in botany species. To gain further insights into the position that caspase-3-like protease activation occupied in the apoptotic signal pathway, two-dimensional gel electrophoresis approaches were utilized. In our study, a total of 15 protein spots affected by caspase-3-like activation were analyzed, including eight proteins up-regulated and other seven proteins down-regulated (Figure 7). Since the activation of caspase led to many cleavage of targeted proteins and inhibition of antiapoptotic factors, these proteins can be involved in apoptotic downstream signal transduction in response to caspase-3-like activation. Interestingly, the tendency of three changed proteins (B, C, D spots) had some differences from that of other 12 spots, which were possible effects of unknown signal proteins modification. In some cases, a functional impact of cleaved targeted proteins have been recognized such as seen with the caspase substrates Rho-GDI2 (Thiede *et al*. 2002; Jin *et al*. 2003), but for most of substrates, the role of protein cleavage was poorly identified. As the total genome sequences of *T. cuspidata* has not been reported, no protein database of *T. cuspidata* could be used to understand the observed proteins. However, our results further showed that activation of caspase-3-like protease affected the development of apoptosis of Ce^{4+}-induced *T. Cuspidata* cells and these protein spots would help to elucidate the caspase-3-like protease role in apoptosis.

In summary, findings of the present study demonstrate that Ce^{4+} at 1 mM is a potent metallic inductor of apoptosis in suspension cultures of *T. cuspidata* cells. The burst of $O_2\cdot-$ and activation of caspase-3-like protease are required

for Ce^{4+}-induced apoptosis and caspase-3-like protease activation, which partially depends upon the levels of $O_2 \cdot -$. Our results further propose that other signal molecules independent of $O_2 \cdot -$ burst may participate in regulating caspase-3-like protease activation. In addition, a total of 15 proteins changed in response to caspase-3-like protease were identified, which pave the way to a better understanding of the mechanisms of Ce^{4+}-induced apoptosis.

Acknowledgement

The authors were very grateful for the financial support from the National Natural Science Foundation of China (Project Nos. 20176038 and 20236040).

References

Balk J, Chew SK, Leaver CJ, Mccabe PF. 2003 The intermembrance space of plant mitochondria contains a Dnase activity that may be involved in programmed cell death. *Plant J* **34**, 573–583.

Beers EP. 1997 Programmed cell death during plant growth and development. C*ell Death Differ* **4**, 649–661.

Buckner B, Johal GS, Janick-Buckner D. 2000 Cell death in maize. *Physiol Plant* **108**, 231–239.

Chen HM, Zhou J, Dai YR. 2000 Cleave of lamin-like proteins in in vivo and in vitro apoptosis of tobacco protoplasts induced by heat shock. *FEBS Lett*. **480**, 165–168.

Chichkova NV, Kim SH, Titova ES *et al*. 2004 A plant caspase-like protease activated during the hypersensitive response. *Plant Cell* **16**, 157–171.

Chung YM, Bae YS, Lee SY. 2003 Molecular ordering of ROS production, mitochondrial changes, and caspase activtion during sodium saliculate-induced apoptosis. *Free Radical Biol Med* **34**, 434–442.

Clarke A, Radhika D, Hurst RD, Hancock JT, Neill SJ. 2000 NO way back: Nitric oxide and programmed cell death in *Arabidopsis thaliana* suspension cultures. *Plant J* **24**, 667–677.

Dat J, Vandenabeele S, Vranaová E, Van Montagu M, Inzé D, Van Breusegem F. 2000 Dual action of the active oxygen species during plant stress responses. *Cell Mol life Sci* **57**, 779–795.

De Jong AJ, Hoeberichts FA, Yakimova ET, Maximova E, Woltering EJ. 2000 Chemical-induced apoptotic cell death in tomato cells: Involvement of caspase-like proteases. *Planta* **211**, 656–662.

De Dong AJ, Yakimova ET, Kapchina VM, Woltering EJ. 2002 A critical role for ethtlene in hydrogen perxide release during programmed cell death in tomato suspension cells. *Planta* **214**, 537–545.

Dellaporta SL, Wood J, Hicks JB. 1983 A plant DNA minipreparation: Version II. *Plant Mol Biol Rep* **1**, 19–23.

Del Pozo O, Lam E. 1998 Caspases and programmed cell death in the hypersensitive response of plants to pathogens. *Curr Biol* **8**, 1129–1132.

Elbaz M, Avni A, Weil M. 2002 Constitutive caspase-like machinery executes programmed cell death in plant cells. *Cell Death Differ* **9**, 726–733.

Ellis RE, Yuan JY, Horvitz HR. 1991 Mechanism and functions of cell death. *Annu Rev Cell Biol* **7**, 663–698.

Ge ZQ, Yuan YJ, Wang YD, Ma ZY, Hu ZD. 2002 Ce^{4+}-induced apoptosis of *Taxus cuspidata* cells in suspensions culture. *J Rare Earths* **20**, 139–144.

Han RB, Yuan YJ. 2004 Oxidative burst in suspension culture of *Taxus cuspidata* induced by a Laminar shear stress in short-term. *Biotechnol Prog* **20**, 507–513.

He X, Kermode AR. 2003 Proteases associated with programmed cell death of megagametophyte cells after germination of white spruce (*Picea glauca*) seeds. *Plant Mol Biol* **52**, 729–744.

He YW, Loh CS. 2000 Cerium and lanthanum promote floral initiation and reproductive growth of *Arabidopsis thaliana*. *Plant Sci* **159**, 117–124.

Jabs T, TschÖpe M, Colling C, Hahlbrock K, Scheel D. 1997 Elicitor-stimulated ion fluxes and $O_2 \cdot -$ from the oxidative burst are essential components in triggering defense gene activation and phytoalexin synthesis in parsley. *Proc Natl Acad Sci* **94**, 4800–4805.

Jin BF, He K, Wang HX *et al*. 2003 Proteomic analysis of ubiquitin-proteasome effects: insight into the function of eukaryotic initiation factor 5A. *Oncogene* **22**, 4819–4830.

Kaji T, Hachimura S, Ise W, Kaminogawa S. 2003 Proteome analysis reveals caspase activation in hyporesponsive CD4 T lymphocytes induced in vivo by the oral administration of antigen. *J Biol Chem* **278**, 27836–27843.

Korthout HAAJ, Berecki G, Bruin W, Duijn BV, Wang M. 2000 The presence and subcellular localization of caspase 3-like proteinases in plant cells. *FEBS Lett* **475**, 139–144.

Levine A, Tenhaken R, Dixon RA, Lamb CJ. 1994 H_2O_2 from the oxidative burst orchestrates the pant hypersensitive disease resistance response as a local trigger of programmed cell death and a diffusible inducer of cellular protectant genes. *Cell* **79**, 583–593.

Li C, Yuan YJ, Ma ZH, Hu ZD, Sun AC, Hu CX. 2002 Cell apoptosis induced by oligosaccharide in suspension cultures of *Taxus chinensis*. *Acta Botanica Sinica* **44**, 598–602.

Mlejnek P, Procházka S. 2002 Activation of caspase-like proteases and induction of apoptosis by isopentenyladenosine in tobacco BY-2 cells. *Planta* **215**, 158–166.

Overmyer K, Tuominen H, Kettunen R *et al*. 2000 Ozone-sensitive *Arabidopsis* rcd1 mutant reveals opposite roles for ethylene and jasmonate signaling pathways in regulating superoxide-dependent cell death. *Plant Cell* **12**, 1849–1862.

Qiao JJ, Yuan YJ, Zhao H, Wu JC, Zeng AP. 2002 Apoptotic cell death in suspension cultures of *Taxus cuspidata* co-treated with salicylic acid and hydrogen peroxide. *Biotechnol Lett* **25**, 387–390.

Ryerson PH, Heath MC. 1996 Cleavage of nuclear DNA into oligonucleosomal framents during cell death induced by fungal infection or abiotic treatments. *Plant Cell* **8**, 393–402.

Simizu S, Takada M, Umezawa K, Imoto M. 1998 Requirements of caspase-3-(-like) protease-mediated Hydrogen Peroxide production for apoptosis induced by various anticancer drugs. *J Biol Chem* **273**, 26900–26907.

Solomon M, Belenghi B, Delledone M, Menachem E, Levine A. 1999 The involvement of cysteine proteases and protease

inhibitors genes in the regulation of programmed cell death in plants. *Plant Cell* **11**, 431–443.

Stohs SJ, Bagchi D. 1995 Oxidative mechanism in the toxicity of metal ions. *Free Rad Biol Med* **18**, 321–336.

Sun Y, Liu DL, Yu ZQ, Zhang Q, Bai J, Sun DY. 2003 An apoplastic mechanism for short-term effects of rare earth elements at lower concentrations. *Plant Cell Environ* **26**, 887–896.

Thiede B, Siejak F, Dimmler C, Rudel T. 2002 Prediction of translocation and cleavage of heterogeneous ribonuclear proteins and Rho guanine nucleotide dissociation inhibitor 2 during apoptosis by subcellular proteome analysis. *Proteomics* **2**, 996–1006.

Tian RH, Zhang GY, Yan CH, Dai YR. 2000 Involvement of poly(ADP-ribose)polymerase and activation of caspase-3-like protease in heat shock-induced apoptosis in tobacco suspension cells. *FEBS Lett* **474**, 11–15.

Wätjen W, Beyersmann D. 2004 Cadmium-induced apoptosis in C6 glioma cells: Influence of oxidative stress. *Biometals* **17**, 65–78.

Wätjen W, Cox M, Biagioli M, Beyersmann D. 2002 Cadmium-induced apoptosis in C6 glioma cells: Mediation by caspase 9-activation. *Biometals* **15**, 15–25.

Yu C, Rahmani M, Dent P, Grant S. 2004 The hierarchical relationship between MAPK signaling and ROS generation in human leukemia cells undergoing apoptosis in response to the proteasome inhibitor bortezomib. *Exp Cell Res* **295**, 555–566.

Yuan YJ, Ge ZQ, Li JC, Wu JC, Hu ZD. 2002a Differentiation of apoptotic and necrotic cells in suspension cultures of *Taxus cuspidata* by the combined use of fluorescent dying and histochemical staining methods. *Biotechnol Lett* **24**, 71–76.

Yuan YJ, Hu GW, Wang CG, Jing Y, Zhou YQ, Shen PW. 1998 Effect of rare earth compounds on the growths, Taxol biosynthesis and release of *Taxus Cuspidata* cell culture. *J Rare Earths* **16**, 56–60.

Yuan YJ, Li JC, Ge ZQ, Wu JC. 2002b Superoxide anion burst and taxol production induced by Ce^{4+} in suspension cultures of *Taxus cuspidata*. *J Mol Catal B: Enzym* **18**, 251–260.

Zuppini A, Baldan B, Millioni R, Favaron F, Navazio L, Mariani P. 2003 Chitosan induces Ca^{2+}-mediated programmed cell death in soybean cells. *New Phytol* **161**, 557–568.